Origin of the bandgap in antiferromagnetic NiS

1999 J. Phys.: Condens. Matter 11 1979

(http://iopscience.iop.org/0953-8984/11/8/011)

J. Phys.: Condens. Matter **11** (1999) 1979–1988. Printed in the UK PII: S0953-8984(99)96096-4

Origin of the bandgap in antiferromagnetic NiS

L Koutti and J Hugel

Laboratoire de Spectrométrie Optique de la Matière, Université de Metz—IPC, 1 boulevard Arago, 57078 Metz Cédex 3, France

Received 21 July 1998, in final form 1 December 1998

Abstract. The paramagnetic and antiferromagnetic densities of states for hexagonal NiS have been calculated within the local spin-density approximation. Three factors act favourably as regards the appearance of a gap in the ordered magnetic phase: the presence of the cubic field, the spin-polarized treatment and the lattice dimensions. The forbidden band is located between the metal d bands and confers a Mott insulating character to NiS. A small reduction in the lattice constants makes the tiny gap disappear. The paramagnetic and antiferromagnetic one-electron energy spectra compare satisfactorily with the photoemission results.

1. Introduction

Hexagonal nickel sulphide exhibits a phase transition when the temperature or pressure is increased. NiS passes from an antiferromagnetic semiconducting state at low temperature to a Pauli paramagnetic metal state at higher temperature [1]. The transition temperature turns out to be around 265 K [2]. An applied pressure of about 20 GPa suppresses the antiferromagnetic phase [3, 4]. Sparks and Komoto [5] pointed out that the transition to the antiferromagnetic state is accompanied by a 2% volume increase due to the lattice expansion. The crystal NiAs structure is maintained during cooling down to room temperature [6, 7]. Optical reflectivity measurements [8] show a strong absorption peak near 0.14 eV in the non-metallic phase. The authors associate the absorption peak with a conventional one-electron bandgap. The reported photoemission spectra [9–11] provide evidence that the overall features in the metallic and non-metallic spectra are not significantly changed. The latter result implies that the modes of organization of the electronic states for the paramagnetic and the antiferromagnetic phases are very close.

The theoretical situation is still controversial, since no definite interpretation as regards the nature of the gap is available. White and Mott [12] attribute the appearance of the gap in the low-temperature phase to a splitting and a narrowing of the Ni e_g bands. The approach supposes a Mott–Hubbard mechanism in which the intra-atomic Coulomb energy U of the 3d-metal electrons competes with their bandwidth W. The model forecasts that a small change in U is able to induce the transition when U and W are close in magnitude. Tyler and Fry [13] used a first-principles tight-binding method and discussed the possibilities for understanding the phase transition in NiS. They conclude that the transition may be explained either within a spin-polarized model or with the localization of the d electrons (the Mott–Hubbard transition). Kasowski [14] proposed an alternative explanation in which the transition may be associated with an average electron–phonon coupling. An augmented-plane-wave band calculation has been presented by Mattheiss [15]. His idea was to add a constant positive potential around

0953-8984/99/081979+10$19.50

one nickel atom bearing a spin moment and a negative potential, equal in magnitude, around the second nickel atom with an opposite moment. This procedure has succeeded in leading to a gap opening at the Fermi energy, and suggests that the one-electron model can be used to describe the antiferromagnetic phase.

In contrast to the above results, those of Fujimori *et al* [10, 11, 16] indicate that the metal–non-metal transition in NiS cannot be explained within band-structure calculations. The main argument advanced against the one-electron picture is the significant broadening of the d band in the antiferromagnetic phase as a result of the exchange splitting. The authors attribute the prominent peak at binding energies between 0 and 3 eV below the Fermi level to $d^8\underline{L}$ final states where $\underline{L}$ stands for a ligand hole. They conclude that like that in NiO, the antiferromagnetic gap in NiS has a S 3p–Ni 3d charge-transfer origin. Thus they exclude the possibility of a Mott–Hubbard correlation gap as suggested in references [12] and [17]. A study of the electronic structure of about thirty transition metal sulphides has been made recently by Raybaud *et al* [18]. The local density approximation (LDA) supplemented with the non-local generalized gradient approximation (GGA) has been used. The main result for the NiAs-type monosulphides (FeS, CoS, NiS) concerns the structure of the transition metal 3d bands. The d states form a broad band with no marked ligand-field splitting, which is explained as being a consequence of the $d_{3z^2-r^2}$ orbital overlap. The calculated band structure of the paramagnetic NiS phase is in agreement with the photoemission spectra [16].

The purpose of the present paper is to clarify the origin of the appearance of the gap at the metal–non-metal transition in NiS by investigating the electronic ground state in the magnetic and non-magnetic phases. The one-electron energy spectra have been calculated with a LSDA-LCAO procedure worked out for NiO [19]. In both compounds, Ni is exposed to an octahedral environment which splits the d levels into t_{2g} and e_g subbands. For NiO, an early spin-polarized calculation [20] has confirmed the validity of the one-electron approach, since a small gap has been obtained and explained as being a result of the ligand-field effect. With regard to the Ni crystal surrounding, it is likely that the one-electron picture applies also to NiS. The applicability of the one-electron theory will be checked, taking into account three factors: the symmetry groups, the exchange splitting and the lattice dimensions. The influence of each factor in the gap formation will be specified.

2. Theoretical considerations

The self-consistent resolution of the Kohn–Sham equations is developed in two stages. The first stage yields atomic-like functions obtained through the resolution of a local Kohn–Sham equation. The potential adopted coincides with the crystal potential inside a muffin-tin sphere and is set equal to a constant elsewhere. The local potential depends upon two parameters: the muffin-tin radius and the constant potential outside. The constant potential is not present in the crystal potential since its role is simply that of ensuring the existence of localized functions. A detailed account is given in reference [19]. The second step yields the electronic density expressed in terms of the crystal eigenstates. These are calculated by solving the LCAO Hamiltonian matrix numerically. In our formalism the atomic-like orbitals attached to each crystal constituent can be modified by varying the constant potential outside the muffin-tin sphere. As a general result, a rise of the barrier height stresses the decay of the function tail but maintains the location of the nodes. These functions serve in the basis expansion of the Bloch functions and have significant effects on the crystal density.

In the antiferromagnetic spin-polarized approach, the electrons for a given spin direction ‘feel’ different exchange potentials when they are located on metal spin-up atoms and metal spin-down atoms. As regards the space groups, the metal with spin up and the metal with

spin down are considered as two different atomic species. Below the transition temperature the magnetic ordering corresponds to a compound of ABS_2 type belonging to the D^3_{3d} space group. Above 265 K the paramagnetic metal phase crystallizes in the NiAs structure with space group D^4_{6h}. Each unit cell contains two metal and two sulphur atoms. The difference appears though the symmetry properties related to the metal atoms. In the antiferromagnetic phase the metal spin-up and spin-down atoms are located on distinct sublattices. In contrast, in the paramagnetic phase the two nickel atoms are both attached to a unique lattice and as a consequence exposed to the same phase factor.

3. Results

Within the hexagonal cell the nickel atoms are located at coordinates (0, 0, 0) and (0, 0, 1/2) and the sulphur at $\pm$(1/3, 2/3, 1/4). The experimental values reported in [5] have been used, with a and c equal to 6.5064 and 10.046 au respectively. The potential radii are determined by making the potential spheres touch for the atoms of the same species. The nickel potentials touch along the c-axis while the sulphur potentials touch along the shortest edge of the distorted octahedron formed by the six sulphurs. The shortest distance joins two sulphurs located in distinct hexagonal planes with a 6.272 au a-value instead of 6.5064 au between two sulphurs

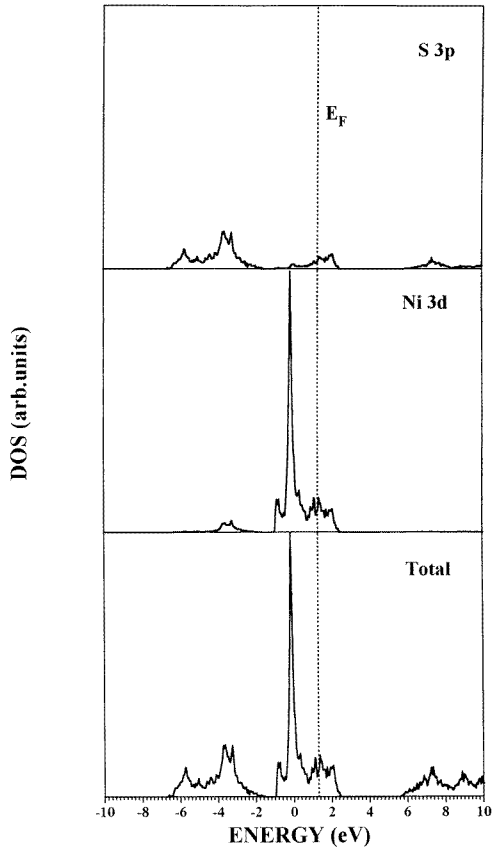

Figure 1. The total and partial ground-state DOS for NiS in the paramagnetic phase.

within the plane. The smallest value is retained for the sulphur potential sphere. The potential spheres overlap between two first-neighbour nickel and sulphur atoms such that the fraction of the unit cell inside the potential spheres amounts to 89%.

The secular matrix is spanned by the 3s and 3p sulphur functions together with the 3d, 4s and 4p metal functions. They generate a 26-by-26-dimensional matrix for both the paramagnetic and antiferromagnetic unit cells. The radii for the metal and sulphur spheres are respectively 2.511 au and 3.136 au. The convergence is considered as achieved once the occupation numbers are stable up to five figures. The following results were obtained with the localizing potentials fixed at 0.8 au for the metal and 0.5 au for the sulphur.

Table 1. Comparison between reliable quantities for several self-consistent results.

	Occupied p bands, p mixing rate (in %)	Occupied d bands, d mixing rate (in %)	Empty d band, d mixing rate (in %)	Gap (in eV)	Ionicity (in e)	Moment (μ_B)
Paramagnetic phase	84.4	93.9	65.8	0.00	1.00	0.00
Antiferromagnetic phase	81.4	92.1	67.0	0.10	1.02	0.86
Uniaxial pressure 3.6%	86.9	90.0	67.0	0.08	1.17	0.80
Hydrostatic pressure 2%	84.4	92.0	66.3	0.00	1.25	0.74
LSDA + U $U = 4$ eV	71.5	43.6	77.8	1.20	1.19	1.54

The paramagnetic density of states calculated with the D^4_{6h}-symmetry Hamiltonian is displayed in figure 1. In order of increasing energy, the bands originating from the 3p sulphur orbitals appear below the bands subspanned by the 3d-metal orbitals. The bands are well identified and provide arguments indicating an ionic nature for NiS. The calculated charge ascribed to one site and the mixing ratios expressed as percentages are summarized in table 1. The departure from the perfect ionicity of two electrons indicates a noticeable p–d mixing, confirmed by a hybridization ratio lower than unity. The density of states is similar to that obtained by Raybaud *et al* [18], except as regards the lack of overlap between the p and d bands in our spectrum. However, the location of the density peaks with respect to the Fermi level and the overall shape of the density curve compare favourably with the experimental photoemission results.

The antiferromagnetic density of states calculated with the expanded lattice parameters (by 1% for c and 0.3% for a [5]) is depicted in figure 2. The occupied p and d one-electron energy states obtained with the D^3_{3d}-symmetry matrix extend over almost the same energy ranges as for the paramagnetic phase. The difference becomes visible in the d-band organization, since the balance between the two d spin directions valid in the paramagnetic phase is now destroyed. As a consequence of the spin polarization, the prominent d paramagnetic peak is divided into two peaks separated by 0.65 eV. The separation of the majority d bands from the minority ones is related to the distinct exchange–correlation potentials acting on each spin direction. The calculated spin moment amounts 0.86 μ_B, to be compared with the known experimental values amounting either to 1.45 μ_B [21] or 1.7 μ_B [2]. The major and interesting result is the opening

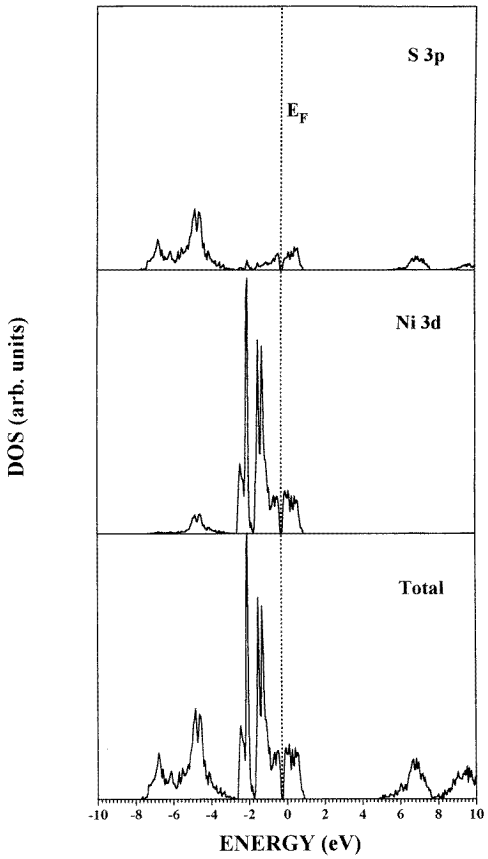

Figure 2. The total and partial ground-state DOS for NiS in the antiferromagnetic phase.

of a small gap (≈0.1 eV) within the minority d band. Since the ionicity has changed only modestly with respect to its value in the paramagnetic phase, its influence on the crystal-field splitting remains negligible. One deduces that the crystal field does not become strong enough to drive the opening of the gap, and that the observed appearance of the gap is due to the spin polarization.

In order to get a deeper insight into the origin of the gap, various simulations have been put forward. A first attempt consists in artificially introducing the spin polarization into the non-magnetic D^4_{6h} matrix. Now the different exchange terms acting on the metal electrons give rise to the appearance of the gap. The opposite case—namely that of the suppression of the spin polarization within the antiferromagnetic D^3_{3d} matrix—leads to the disappearance of the gap. For the two (D^4_{6h} and D^3_{3d}) symmetries, the absence of the spin polarization leads to a metallic behaviour. This demonstrates clearly that the spin-polarized approach with its specific treatment for each spin direction is the main factor that governs the emergence of the forbidden band.

To complete our investigations, the influence of the lattice dimensions has been considered too. This factor has been taken into account in view of the experimental fact [3, 4] that a high pressure removes the gap. Within the hypothesis that the pressure shrinks the lattice constants, two kinds of modification have been imposed. An axial pressure modelled by a reduction of

the sole c-parameter makes the gap disappear when the constant is shortened by up to 3.9%. In contrast, a hydrostatic pressure characterized by a uniform decrease of all of the parameters causes the gap to vanish, since there is a 1.9% shortening. Taking into account the volume, it undergoes a reduction of only 3.9% in the former case and a decrease reaching 5.7% in the latter. One deduces that the gap is more easily removed for uniaxial pressure and that the gain in overlap between the p and d orbitals is sufficient to eliminate the gap. Even if the existence of the gap can only be demonstrated within the spin-polarized approach, the equilibrium lattice constants favour its occurrence.

4. Discussion

The d states are exposed to the crystal-field effect generated by a deformed octahedron of six sulphur atoms. The classical ligand-field model casts the crystal d states into a triply degenerate t_{2g} band subspanned by the eigenfunctions

$$3z^2 - r^2 \qquad \sqrt{\frac{2}{3}}xy + \frac{1}{\sqrt{3}}yz \qquad -\frac{1}{\sqrt{3}}zx + \sqrt{\frac{2}{3}}(x^2 - y^2)$$

and a doubly degenerate e_g band with the combinations

$$\frac{1}{\sqrt{3}}xy - \sqrt{\frac{2}{3}}yz \qquad \sqrt{\frac{2}{3}}zx + \frac{1}{\sqrt{3}}(x^2 - y^2).$$

For a distorted octahedron like that in the NiAs structure, the t_{2g} states split further into a low-lying $3z^2 - r^2$ state and two remaining doubly degenerate higher-energy states. The expressions for the eigenfunctions result from the choice of the coordinate system, where the z-axis was taken parallel to the hexagonal c-direction.

The interpretation of the complete set of results is based on the analysis of the partial d densities of states in the antiferromagnetic phase presented in figure 3. The identification of the metal d bands has been achieved with the help of the calculated total charge versus energy. With increasing energy, the majority t_{2g} band occupies an energy interval between -2.7 and -1.9 eV and the e_g band an interval ranging from -1.9 eV to -0.3 eV. The minority t_{2g} band spreads over the same energy range as the majority e_g band. The minority e_g band extends from -0.2 eV to 1 eV on the energy scale. Schematic representations of both the paramagnetic and antiferromagnetic densities of states are pictured in figure 4. The clear assignment of the various bands shows that the forbidden band appears in between bands predominantly of d character. Consequently the gap in NiS can be termed an exchange–correlation gap. NiS exhibits a limiting case for which the spin splitting and the cubic-field separation are of the same order of magnitude. This situation explains the existence of the forbidden band, since there is a separation between the minority t_{2g} and e_g bands. The emergence of the gap in NiS is possible owing to the constructive combination of three factors: the presence of the cubic field, the spin-polarized approach and also the lattice dimensions. Nevertheless, our findings cannot ascribe the origin of the gap formation to the observed lattice expansion at the transition.

The shortening of the forbidden bandwidth induced under the pressure simulations finds a simple explanation when the partial d densities are examined. Inspection of figure 3 shows that the minority t_{2g} and e_g bands lie on both sides of the Fermi level. The dispersion of the bands depends upon the magnitude of the two centre integrals. As a general rule, a rise in the orbital overlap enlarges the allowed bandwidths. Following Slater and Koster [22], the p–d and the d–d interactions can be expressed in terms of the well known σ-, π- and δ-integrals with $|\mathrm{dd}\sigma| \geqslant |\mathrm{dd}\pi| \geqslant |\mathrm{dd}\delta|$ on one hand and $|\mathrm{pd}\sigma| \geqslant |\mathrm{pd}\pi|$ on the other. A compression along the c-axis affects the σ-type integrals whereas the π-type integrals are sensitive to a contraction

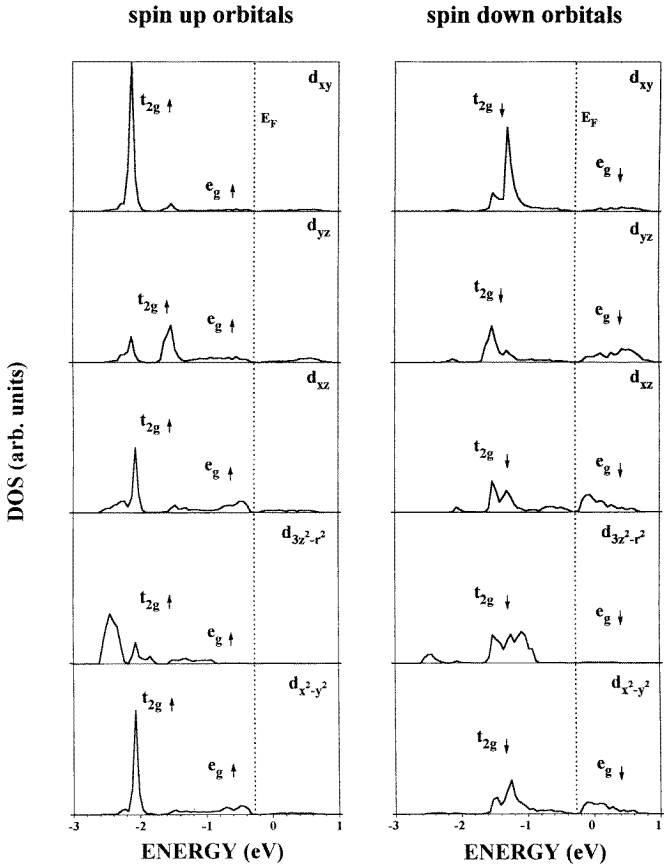

Figure 3. The d partial ground DOS for NiS in the antiferromagnetic phase.

in the a-direction. The t_{2g} and e_g widenings generated by the overlap increase according to the integrals involved. Thus a uniform compression implies considering all of the standard integrals, in contrast to the c-compression for which only the σ-integrals have to be considered. Since the σ-integrals are the largest in magnitude, the uniaxial reduction fills the gap more efficiently than does the tridimensional reduction for an equal change in volume. The crystal compression is accompanied by an increase of the ionicity and a reduction of the moments, according to the results reported in table 1. The explanation comes from the reorganization of the DOS that can be inferred from the occupation ratios. The modifications are coherently interpreted in terms of a loss of occupied majority d states compensated for by a gain of p states within the sulphur p band.

The spin polarization does not separate the majority from the minority d states in one stage. The shift is accompanied by a change in the distribution of the p and d states within the bands, as illustrated by the mixing rates given in table 1. As the ionicities in the paramagnetic and antiferromagnetic phases show very close values, the entire occupied p and d levels remain practically unchanged. Now a fraction of the p states are lifted towards higher energies and substituted for minority d states. The released low-energy p states are filled up with majority d states, giving rise to unbalanced majority and minority d levels. The calculated magnetic moment is lower than the experimental value, but a possible way to find a value closer to

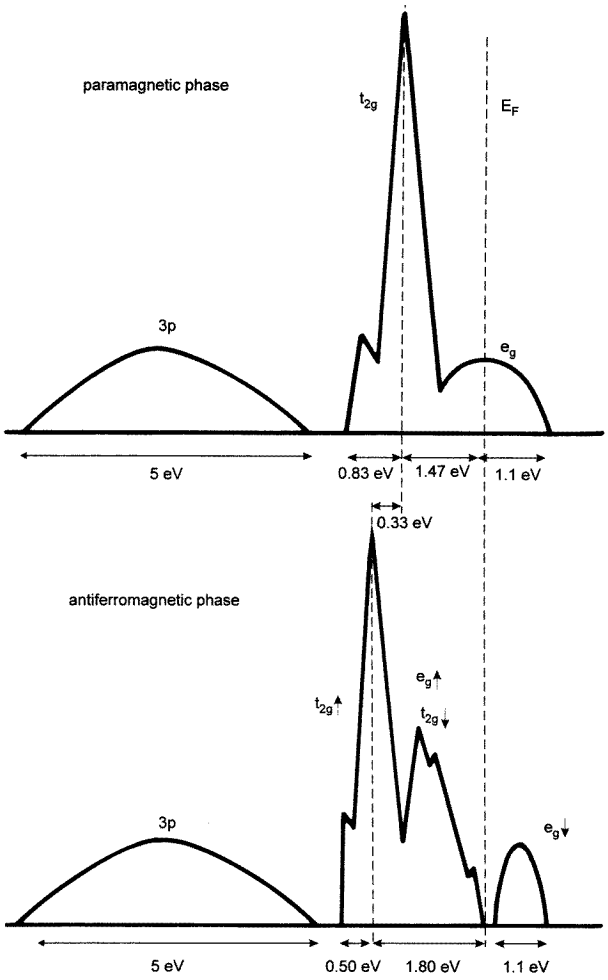

Figure 4. Comparison of the schematic total ground-state DOS for NiS in the paramagnetic and antiferromagnetic phases. The main d peak shifts 0.33 eV downwards at the metal–non-metal transition.

the experimental ones is to use the LSDA + U correction [23]. It is known from a previous study devoted to NiO that the introduction of the correlation energy U widens the gap and increases the moment. The two quantities vary in the right way for NiO. If the same approach is applied to NiS, the agreement with the experimental moment will be improved but the accordance with the gap width will be lessened. Ascribing a value of 4 eV to U leads to a spin moment amounting to 1.54 μ_B and a gap reaching 1.2 eV. The higher gap value is prevented from disappearing when a small reduction of the lattice is considered. It turns out that the LSDA + U treatment does not provide the full answer, especially when one focuses on the forbidden band.

The calculated paramagnetic and antiferromagnetic densities of states do not look identical as in the experimental situation [16]. The clear difference concerns the position of the main d peak with respect to the Fermi level. According to the calculations, the d peak is pushed downwards towards lower energies by 0.33 eV, while the experimental spectra show barely a

0.05 eV displacement. Obviously the spin-polarized DOS cannot fit with the non-polarized DOS owing to the difference in their exchange potentials. That argument has been invoked by Fujimori *et al* [16] to claim that a band description fails to explain the gap. In fact the spin splitting is not as large as 2 eV, but is only 0.8 eV, and also the overall occupied energy ranges remain unchanged in the two phases. The departure from the experiment reaches about 0.3 eV, which can be considered as a satisfactory agreement within the simple LSDA approach.

For the paramagnetic phase the agreement between the one-electron model and the experimental results can be considered as well established. The ability of the band theory to adequately describe the paramagnetic spectral lines was first pointed out by Fujimori *et al* [11] and received further confirmation from the work of Raybaud *et al* [18] and ours. The configuration interaction cluster model derived for the ordered magnetic phase describes the paramagnetic phase just as well. Both approaches successfully reproduce the prominent peak at the binding energies ranging from 0 to 3 eV. Contrary to the case for the paramagnetic phase, the situation for the antiferromagnetic phase is under debate. The failure of the LAPW antiferromagnetic solution [11] cannot be taken as a definite argument against the one-electron model. Here, a converged antiferromagnetic solution has been performed, whose energy band density is satisfactory as regards the intensity of the main peak but not as regards its location with respect to the Fermi level. Another difference is that the band theory and the cluster model do not ascribe the same character to the highest occupied states. The top of the valence band is p sulphur-like according to the configuration interaction calculations reported in reference [11]. Our band calculations show mixed p–d states for the upper valence band, the proportion of the p sulphur states amounting to 25%. The low degree of p hybridization present in the high-lying valence states may explain the modest moment, which is too small by almost a factor of two. The difficulties related to the peak location and to the moment value are not due to the band theory itself but rather to the mean-field character of the local density approximation.

5. Conclusions

The band approach can be used to investigate the NiS phase transition since it provides evidence regarding the factors playing a part in the gap formation. The paramagnetic density of states presents a satisfactory agreement with recent self-consistent calculations and with the experimental photoemission spectra. The results for the antiferromagnetic phase are acceptable even if they do not fully reproduce the experimental density of states and the magnetic moment. NiS is an interesting compound which demands further theoretical developments in order to reconcile the theory with the experimental results.

References

[1] Sparks J T and Komoto T 1967 *Phys. Lett.* A **25** 398
[2] Sparks J T and Komoto T 1968 *Rev. Mod. Phys.* **40** 752
[3] Anzai S and Ozawa K 1970 *J. Appl. Phys.* **41** 3558
[4] Kosyreva M S, Novikov V N and Tallerchik B A 1972 *Sov. Phys.–Solid State* **14** 639
[5] Sparks J T and Komoto T 1963 *J. Appl. Phys.* **34** 1191
[6] Trahan J, Goodrich R G and Watkins S F 1970 *Phys. Rev.* B **2** 2859
[7] McWhan D B, Marezio M, Remeika J P and Dernier P D 1972 *Phys. Rev.* B **5** 2552
[8] Barker A S Jr and Remeika J P 1974 *Phys. Rev.* B **10** 987
[9] Hüfner S and Wertheim G K 1991 *Phys. Lett.* B **44** 1364
[10] Fujimori A, Matoba M, Anzai S, Terakura K, Taniguchi M, Ogawa S and Suga S 1987 *J. Magn. Magn. Mater.* **70** 67
[11] Fujimori A, Terakura K, Ogawa S, Taniguchi M, Suga S, Matoba M and Anzai S 1988 *Phys. Rev.* B **37** 3109
[12] White R M and Mott N F 1971 *Phil. Mag.* **24** 845

[13] Tyler J M and Fry J L 1970 *Phys. Rev.* B **1** 4604
[14] Kasowski R V 1973 *Phys. Rev.* B **8** 1378
[15] Mattheiss L F 1974 *Phys. Rev.* B **10** 995
[16] Fujimori A, Namatame H, Matoba M and Anzai S 1990 *Phys. Rev.* B **42** 620
[17] Koehler R F and White R L 1973 *J. Appl. Phys.* **44** 1682
[18] Raybaud P, Hafner J, Kresse G and Toulhoat H 1997 *J. Phys.: Condens. Matter* **9** 11 107
[19] Hugel J and Kamal M 1997 *J. Phys.: Condens. Matter* **9** 647
[20] Terakura, Oguchi T, Williams A R and Kübler J 1984 *Phys. Rev.* B **30** 4734
[21] Coe J M D, Brusetti R, Kallel A, Schweizer J L and Fuess H 1974 *Phys. Rev. Lett.* **32** 1257
[22] Slater J C and Koster G F 1954 *Phys. Rev.* **94** 1498
[23] Anisimov V I, Zaanen J and Andersen O K 1991 *Phys. Rev.* B **44** 943